Exchange coupling in Bi$_2$Se$_3$/EuSe heterostructures and evidence of interfacial antiferromagnetic order formation

Ying Wang,[1] Valeria Lauter,[2,*] Olga Maximova,[1] Shiva T. Konakanchi,[1] Pramey Upadhyaya,[3] Jong Keum,[2,4] Haile Ambaye [2], Jiashu Wang [5], Maksym Zhukovskyi,[6] Tatyana A. Orlova,[6] Badih A. Assaf,[5] Xinyu Liu,[5] and Leonid P. Rokhinson [1,3,7,†]

[1]*Department of Physics and Astronomy, Purdue University, West Lafayette, Indiana 47907, USA*

[2]*Neutron Scattering Division, Neutron Sciences Directorate, Oak Ridge National Laboratory, Oak Ridge, Tennessee 37831, USA*

[3]*Elmore Family School of Electrical and Computer Engineering, Purdue University, West Lafayette, Indiana 47907, USA*

[4]*Center for Nanophase Materials Sciences, Physical Science Directorate, Oak Ridge National Laboratory, Oak Ridge, Tennessee 37831, USA*

[5]*Department of Physics and Astronomy, University of Notre Dame, Notre Dame, Indiana 46556, USA*

[6]*Notre Dame Integrated Imaging Facility, University of Notre Dame, Notre Dame, Indiana 46556, USA*

[7]*Birck Nanotechnology Center and Purdue Quantum Science and Engineering Institute, Purdue University, West Lafayette, Indiana 47907, USA*

Spatial confinement of electronic topological surface states (TSSs) in topological insulators poses a formidable challenge because TSSs are protected by time-reversal symmetry. In previous works formation of a gap in the electronic spectrum of TSSs has been successfully demonstrated in topological insulator/magnetic material heterostructures, where ferromagnetic exchange interactions locally lift the time-reversal symmetry. Here we report experimental evidence of exchange interaction between a topological insulator Bi$_2$Se$_3$ and a magnetic insulator EuSe. Spin-polarized neutron reflectometry reveals a reduction of the in-plane magnetic susceptibility within a 2 nm interfacial layer of EuSe, and the combination of superconducting quantum interference device (SQUID) magnetometry and Hall measurements points to the formation of an interfacial layer with a suppressed net magnetic moment. This suppressed magnetization survives up to temperatures five times higher than the Néel temperature of EuSe. Its origin is attributed to the formation of an interfacial antiferromagnetic state. Abrupt resistance changes observed in high magnetic fields are consistent with antiferromagnetic domain reconstruction affecting transport in a TSS via exchange coupling. The high-temperature local control of TSSs with zero net magnetization unlocks new opportunities for the design of electronic, spintronic, and quantum computation devices, ranging from quantization of Hall conductance in zero fields to spatial localization of non-Abelian excitations in superconducting topological qubits.

I. INTRODUCTION

Topologically protected gapless surface states (TSSs) are both a distinctive feature and a curse of topological insulators (TIs) [1]: on the one hand, these states are robust against local disorder; on the other hand, they cannot be shaped by conventional lithographic techniques. A gap in the electronic spectrum of TSSs can be induced by breaking time-reversal symmetry, e.g., by applying strong magnetic fields. Time-reversal symmetry can be spontaneously broken in a magnetic topological insulator: the quantum anomalous Hall effect, a hallmark of broken time-reversal symmetry, has been observed both in intrinsic [2] and conventional magnetically doped TIs [3]. The disadvantages of bulk doping include the global gapping of TSSs, uneven band gaps across the TSS due to inhomogeneous distribution of dopants, formation of impurity bands, and high density of lattice defects [4]. The magnetic proximity effect [5] is an attractive alternative to break time-reversal symmetry which

alleviates the aforementioned drawbacks. There are a number of works where the anomalous Hall effect has been reported in TI/magnetic insulator (TI/MI) heterostructures [6–17], including TI/antiferromagnetic insulators [18,19]. In all these heterostructures the magnetic exchange interaction induces out-of-plane ferromagnetic spin arrangement at the TI/MI interface; the exchange field breaks time-reversal symmetry and opens a gap in the TSS spectrum.

One of the most studied TI/MI systems is EuS/Bi$_2$Se$_3$, where a combination of polarized neutron reflectometry (PNR) and superconducting quantum interference device (SQUID) magnetometry revealed interfacial magnetization that survives up to room temperature, a 20-fold enhancement of Curie temperature compared to the $T_c = 17$ K in bulk EuS [12]. Subsequent studies by x-ray magnetic circular dichroism [20] or low energy muon spin rotation experiments [21,22] failed to detect an enhancement of interfacial T_c, most likely due to a low sensitivity or inadequate spatial resolution of these methods. Theoretically, the enhancement of the magnetic order was attributed to the presence of a strong spin-orbit coupling in the TI [23]; however *ab initio* calculations produced contradictory results. Kim *et al.* [24] found that TSSs in Bi$_2$Se$_3$ can contribute to exchange coupling of Eu moments
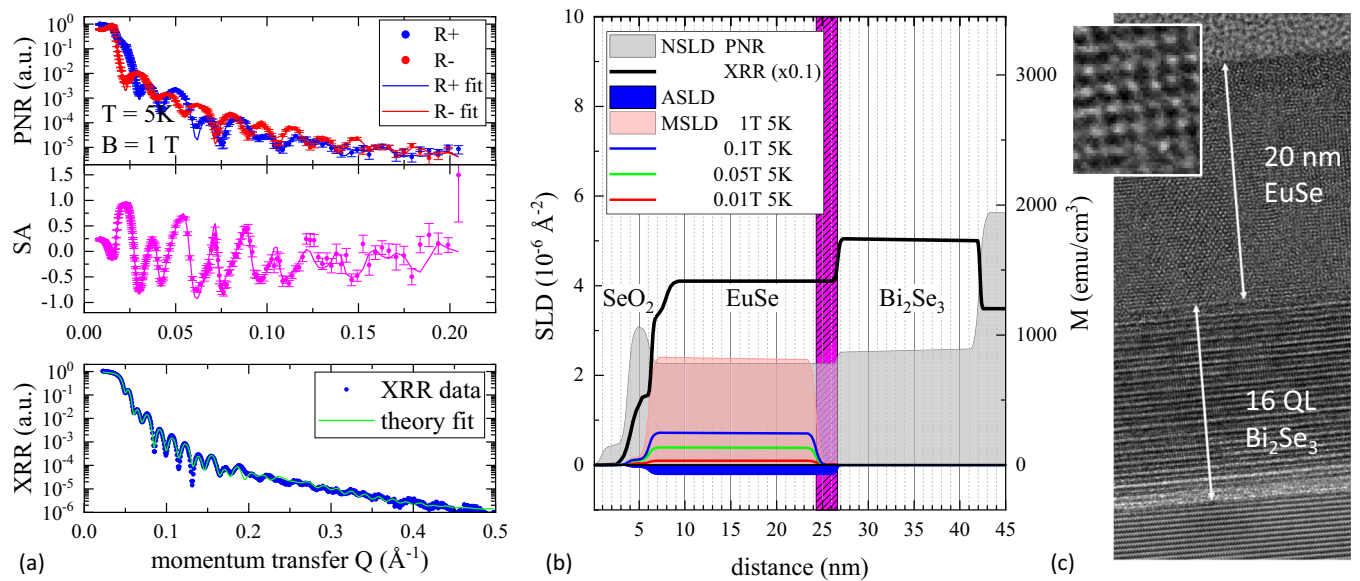
*lauterv@ornl.gov
†leonid@purdue.edu

FIG. 1. Polarized neutron reflectometry (PNR). (a) PNR data for spin-up (R^+) and spin-down (R^-) neutrons (top panel), spin-asymmetry ratio $SA = (R^+ - R^-)/(R^+ + R^-)$ (middle panel), and x-ray reflectometry (XRR) data (bottom panel) are plotted as a function of the wave vector transfer $Q = 4\pi \sin\theta/\lambda$ (where θ is the incident angle and λ is the neutron wavelength). Solid lines are fits to the data; error bars represent corresponding standard deviations. (b) PNR nuclear (NSLD, gray), magnetic (MSLD), and absorption (ASLD, blue) scattering length density (SLD) profiles are plotted as a function of the distance from the sample surface. The red, green, and magenta solid lines, as well as pink area, show MSLD profiles at $H = 0.01$, 0.05, 0.1, and 1 T. The right scale is MSLD converted to volume magnetization. The interfacial layer of EuSe where magnetization is suppressed is highlighted with a magenta color. (c) High-resolution transmission electron microscopy image of the sample.

through the RKKY mechanism that results in the enhancement of T_c at the EuS/Bi$_2$Se$_3$ interface. It was also argued that interdiffusion of Eu across the interface may induce magnetic moments on neighboring Se and Bi atoms an order of magnitude larger than the substrate-induced moments [25]. On the contrary, a recent first-principles density functional study [26] did not find either additional induced magnetization at the interface or the magnetic proximity effect and a gap opening in electronic spectrum of TSSs. Instead, the calculations revealed a downshift of energy states by 0.4 eV and relocation of TSSs to the second quintuple layer due to partial charge transfer from Eu to Se and a dipole formation at the interface. Theoretical difficulties arise from the complex nature of the magnetic interactions in europium compounds [27]. Experimentally, effective magnetic proximity coupling requires a clean, sharp, and controlled interface between a magnetic insulator and a TI due to the extreme short-range nature of the exchange interaction.

In this work we study interfacial exchange in Bi$_2$Se$_3$/EuSe heterostructures using a combination of PNR, SQUID magnetometry, and electronic transport measurements. We present experimental evidence of a suppressed magnetization at the Bi$_2$Se$_3$/EuSe interface, which we attributed to the formation of an interfacial antiferromagnetic spin arrangement. An abrupt switching behavior in the magnetoresistance is consistent with domain switching in the antiferromagnetic (AFM) layer. The use of AFM materials to modify electronic transport through TSS states can be particularly advantageous for spatial confinement of non-Abelian excitations, since the zero net AFM magnetization enables small B_{C1} superconductors to be used in close proximity to a magnetic insulator.

II. Bi$_2$Se$_3$/EuSe HETEROSTRUCTURES

EuSe is an antiferromagnetic member of the Eu chalcogenides family with bulk Néel temperature $T_N = 4.6$ K [28]. Near cancellation between nearest and next-nearest neighbor interactions results in a rich magnetic phase diagram which includes antiferromagnetic (AFM), ferrimagnetic (FiM), and ferromagnetic (FM) phases. Eu spins lay within the (111) planes where they are coupled ferromagnetically, and AFM, FiM, and FM phases refer to the mutual orientation of (111) planes. Thin EuSe films grown on Bi$_2$Se$_3$ using molecular beam epitaxy prefer (001) crystal orientation and their magnetic phase diagram is found to be similar to the bulk material [29,30]. For this study, 20 nm of EuSe has been epitaxially grown on Bi$_2$Se$_3$. The materials form a sharp interface as evident from high-resolution transmission electron microscopy (HRTEM) images, Fig. 1(c). While Bi$_2$Se$_3$ grows as a monocrystal over a large surface, EuSe forms a domain structure with characteristic size 15–30 nm; see extended HRTEM images in [30]. From the temperature dependence of magnetic susceptibility at zero magnetic field $T_N \approx 4.4$ K is obtained. It has been previously shown that the Néel temperature of EuSe thin films is very sensitive to biaxial strain [31] and we conclude that EuSe films grown on Bi$_2$Se$_3$ are almost unstrained. At $H \sim 20$ mT the AFM-FiM transition is observed (the exact value depends on the direction of the magnetic field sweep); the film is in a FM phase above 0.2 T (see Ref. [29] and Fig. S3 in [30]). This rich phase diagram allows investigation of the dependence of interfacial exchange interactions on the magnetic phase in the bulk of the EuSe film.
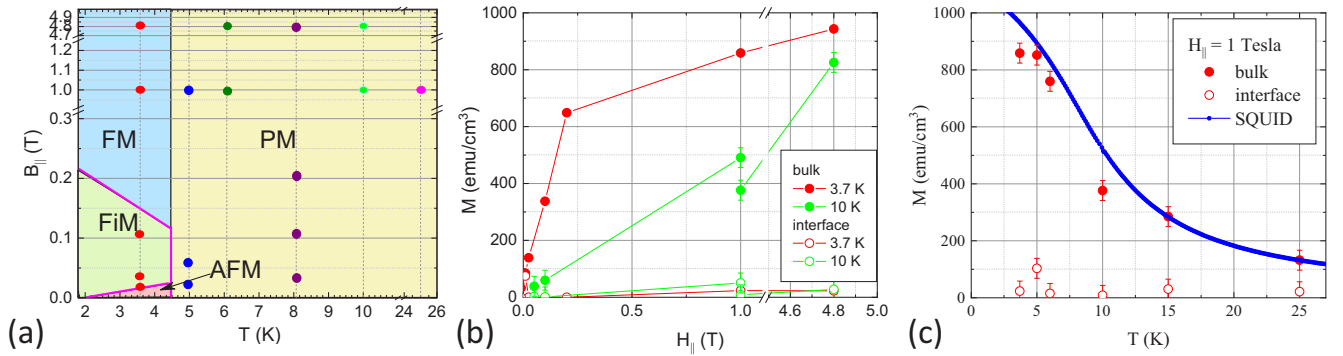
FIG. 2. Temperature and field dependence of in-plane magnetization. (a) Phase diagram of a EuSe thin film obtained using SQUID magnetometry (magenta lines) includes antiferromagnetic (AFM), ferrimagnetic (FiM), ferromagnetic (FM), and paramagnetic (PM) phases. Color dots mark positions of PNR measurements. (b), (c) Magnetic field and temperature dependence of bulk and interfacial in-plane magnetization extracted from PNR measurements. Overall magnetization measured using SQUID magnetometer is shown by a blue line. In (b) two sets of data at 10 K (0–1 T and 1–4.8 T) were taken 1 year apart and reflect small reduction of EuSe film magnetization with time. Note breaks in horizontal and vertical axes in plots (a) and (b).

A. Polarized neutron reflectometry

We apply a method of polarized neutron reflectometry (PNR) as a unique tool that provides high resolution of chemical composition and depth profile of the in-plane magnetization vector and, thus, can probe structure and magnetization at a buried interface. PNR data of Bi$_2$Se$_3$/EuSe film measured in the presence of in-plane external magnetic field $H_\parallel = 1$ T at $T = 5$ K (paramagnetic phase of the bulk EuSe) are shown in Fig. 1(a). There is a visible difference in R^+ and R^- reflectivities for neutrons with spins aligned parallel or antiparallel to the applied magnetic field (R^+ and R^-, respectively). In order to improve precision in the interface depth determination x-ray reflectivity (XRR) measurements were performed on the same sample at room temperature. The fit to the data was performed simultaneously for the PNR and XRR data. The depth profiles of the nuclear and magnetic scattering length densities (NSLD and MSLD), obtained from the fit to the data, correspond to the depth profile of the chemical and in-plane magnetization vector distributions, respectively.

The middle panel in Fig. 1(a) shows the spin asymmetry ratio $SA = (R^+ - R^-)/(R^+ + R^-)$ obtained from the experimental and fitted reflectivity profiles. The SA signal evidences the presence of a depth-dependent magnetic moment. Positions of Bi$_2$Se$_3$/EuSe and Bi$_2$Se$_3$/sapphire interfaces are determined from the NSLD profile and found to be consistent with HRTEM images of the sample cross section. NSLD shows ≈10% contrast between scattering on Bi$_2$Se$_3$ and EuSe with a 1 nm transition region consistent with the PNR depth resolution. The accuracy of the Bi$_2$Se$_3$ interface determination is further improved and confirmed through the analysis of the absorption scattering length density (ASLD), which comes solely from scattering on Eu atoms [32]. Both PNR and HRTEM data reveal a sharp Bi$_2$Se$_3$/EuSe interface; the interfacial roughness obtained from the fit of the PNR and XRR data is 0.6 ± 0.4 nm, extending 1 monolayer into EuSe and less than 1 quintuple layer into Bi$_2$Se$_3$.

The evolution of the MSLD profile, which represents the depth distribution of in-plane magnetization, is shown

in Fig. 1(b) for various values of magnetic field $H_\parallel = 0.01, 0.05, 0.1$, and 1 T. The gradual increase in the bulk magnetization with magnetic field is consistent with the EuSe film being in the paramagnetic state at $T = 5$ K; the magnetization saturates at $M_0 \approx 7\mu_B$ per atom, where μ_B is the Bohr magneton, for $B > 0.2$ T. At the same time there is a distinct suppression of magnetization in EuSe within 2 ± 0.6 nm from the interface. Note that this region is clearly within the EuSe layer according to both ASLD and NSLD data, as is highlighted with a vertical shaded area in Fig. 1(b). To investigate further this feature, we performed PNR measurements in a broad range of magnetic fields and temperatures; see Fig. 2 and extended data in [30]. From a detailed analysis of PNR data it follows that the suppression of the interfacial magnetization is independent of the magnetic state of EuSe film: the data, collected at 3.7 K, span AFM, FiM, and FM phases of the bulk of the film, while the data collected at 10 K correspond to the PM phase. In Fig. 2(b) magnetization (M) in the bulk and in the interfacial layer of the EuSe film is plotted as a function of in-plane magnetic field. At $T = 3.7$ K the bulk M reaches the FiM state ($\sim\frac{1}{3}M_0$) at $H_\parallel \approx 0.1$ T and >90% of M_0 at $H_\parallel = 4.8$ T. The interfacial M remains $<0.1M_0$ in the whole range of magnetic fields available during the PNR experiments. In Fig. 2(c) we plot magnetization in the bulk of EuSe film and in the interfacial layer measured at $H = 1$ T. The bulk magnetization gradually decreases with temperature at $T > T_N$, while the interfacial magnetization remains close to the noise level up to at least 25 K, five times the Néel temperature of the bulk EuSe.

The sharpness of Bi$_2$Se$_3$/EuSe interface over the whole macroscopic sample, revealed by PNR, XRR, and HRTEM, combined with 0.5 nm depth resolution of the PNR technique [33,34] and a clear separation between MSLD signal suppression and NSLD/XRR interfacial boundary, excludes surface roughness and/or intermixing at the Bi$_2$Se$_3$/EuSe interface as a possible reason for the magnetization reduction near the interface. Alternative scenarios for spin arrangement with zero net in-plane magnetization include (i) the formation of an out-of-plane ferromagnetic state or (ii) the formation of an antiferromagnetic state. The thickness of the interfacial layer
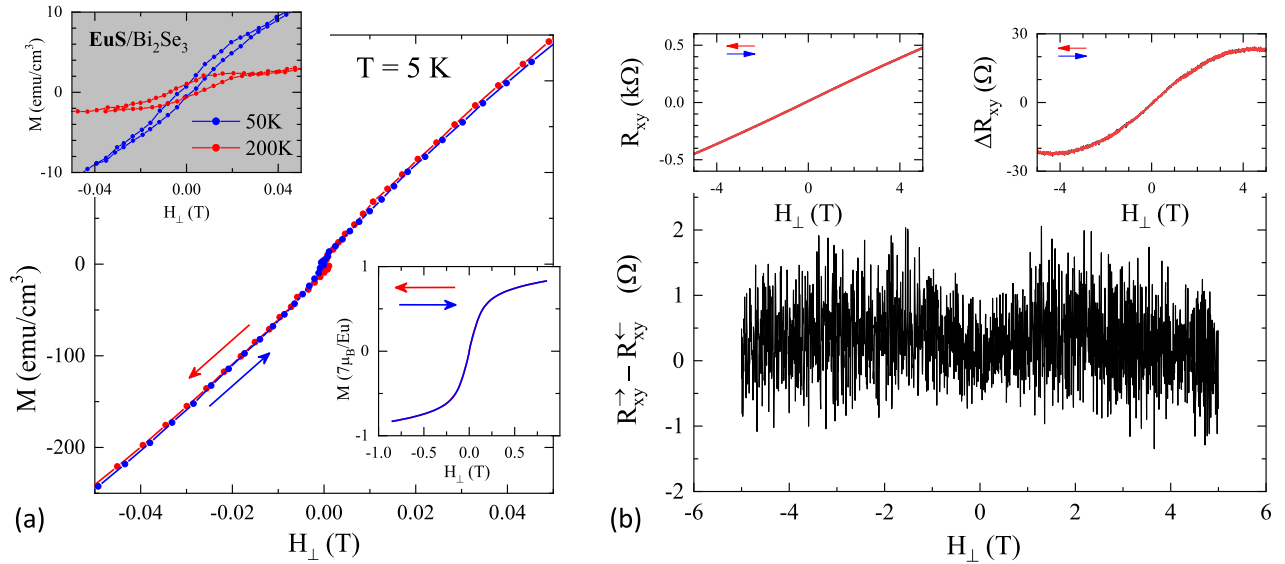
FIG. 3. Out-of-plane magnetization studies. The magnetization and Hall measurements were performed on the $Bi_2Se_3/EuSe$ sample at 5 K, the paramagnetic phase for the bulk EuSe. (a) The out-of-plane magnetization as a function of magnetic field is measured using SQUID magnetometer. The paramagnetic response of EuSe is clearly seen in the enlarged $H_\perp$ range in the lower right inset. The inset with a gray background reproduces the data for EuS/Bi_2Se_3 films taken from Ref. [12] which shows pronounced hysteresis. (b) The difference between Hall resistances measured for two sweep directions shows no hysteresis. The Hall resistance (R_{xy}) and the Hall resistance with a linear component subtracted (ΔR_{xy}) are plotted in the insets.

is $\approx$10% of the total thickness of the EuSe film and in the case in which a ferromagnetic layer is formed near the interface we expect this layer to account for 10% of the saturation magnetization of 1100 emu/cm^3 (4.5×10^{-4} emu for our sample), well within the 10^{-8} emu resolution of the SQUID magnetometer. Indeed, in EuS/Bi_2Se_3 films hysteresis is clearly observed in the magnetization loops in the paramagnetic EuS phase up to 200 K; this hysteresis is considered unambiguous evidence that a ferromagnetic state is formed at the interface [12]. Magnetization loops of $Bi_2Se_3/EuSe$, measured at $T =$ 5 K, are shown in Fig. 3(a), where no hysteresis is observed within a resolution of a few emu/cm^3. For a ferromagnetic EuSe layer 2 nm thick we expect a loop with a magnetization amplitude of 50–100 emu/cm^3. The absence of hysteresis in magnetization loops in $EuSe/Bi_2Se_3$ is contrasted with a pronounced hysteresis in EuS/Bi_2Se_3 reported in Ref. [12] and is consistent with prior studies of $Bi_2Se_3/EuSe$ [35]. The lack of magnetization response to the in-plane magnetic field measured by PNR and an absence of an out-of-plane ferromagnetic state points to the formation of an antiferromagnetic state at the interface.

We note that the Hall resistance also shows no hysteresis, see Fig. 3(b), which indicates that no ferromagnetic state is formed at the interface. We observe an anomalous Hall effect (AHE) [inset in Fig. 3(b)], which most likely originates from the magnetization of EuSe in the bulk. A similar AHE was observed in EuS/Bi_2Se_3 samples [12].

B. Electrical transport

As we show below, the magnetotransport data further corroborate the formation of an antiferromagnetic state. The electronic parameters of the Bi_2Se_3 film were determined by

measuring a sample in the Hall bar geometry. At $T = 5$ K we found the sheet electron density $n = 8.6 \times 10^{12}$ cm^{-2} and mobility $\mu = 470$ cm^2/V s, at $T = 50$ mK, $n = 7.4 \times 10^{12}$ cm^{-2}, and $\mu = 650$ cm^2/V s. Fitting negative magnetoresistance by the Hikami-Larkin-Nagaoka [36] formula we obtained a phase coherence length $l_\phi = 117$ nm at $T = 5$ K and $l_\phi = 485$ nm at $T = 50$ mK.

In Fig. 4(a) we plot magnetoresistance measured in a mesoscopic device. Enhancement of conductivity at low magnetic fields is due to weak antilocalization, and smooth slow reduction of conductivity is expected at higher fields. Unexpectedly, several sharp features are observed at high fields $H > 2$ T for both in-plane $H_\parallel$ and out-of-plane $H_\perp$ field directions. These fields are much larger than $\approx$0.2 T needed to fully saturate magnetization in the bulk of the EuSe film. These sharp magnetoresistance features are abrupt and hysteretic, as seen in the zoomed data. Qualitatively, these observed features are reminiscent of resistance jumps in mesoscopic magnetic materials where field-induced reconstruction of magnetic domains affects the current path. The temperature dependence for one such switching event, measured for the up-sweep of magnetic field, is analyzed in Figs. 4(b) and 4(c). Both the amplitude and the width of the switching approximately follow the temperature dependence of the mean field magnetization $M(T)/M(0) = B_s[3S/(S + 1) \times T_c/T \times M(T)/M(0)]$, where B_s is the Brillouin function. $M(T)/M(0)$ is plotted as a gray line in (c) where we used $S = 7/2$ and $T_c = 1.5$ K. This temperature scaling reiterates the magnetic origin of the switching events.

Epitaxial EuSe films are very resistive: when a vertical voltage ±0.1 V is applied across the 20 nm film using millimeter-sized contacts the leakage current does not exceed 0.5 nA. The EuSe film forms a multidomain structure with
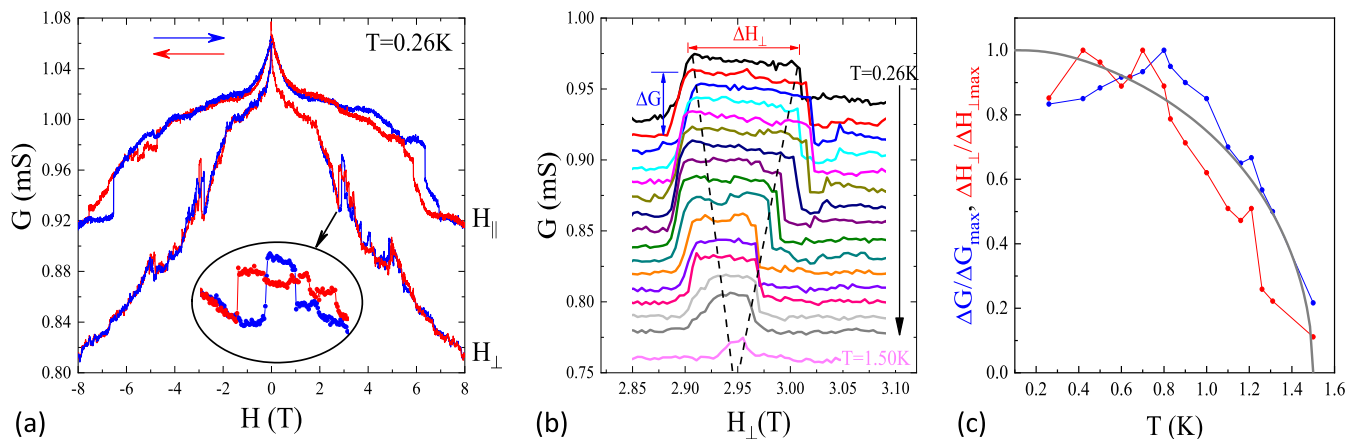
FIG. 4. Sharp switching of sample conductance at high magnetic fields. (a) Two-terminal conductance G of a microscopic sample 1 μm × 2 μm is plotted as a function for in-plane ($H_\parallel$, top curves) and out-of-plane ($H_\perp$, bottom curves) magnetic fields. In the inset a small region with sharp changes of G is zoomed in. (b) Temperature dependence of the sharp switching near $H_\perp = 2.95$ T for the sweep-up direction. The curves are offset by -0.01 mS relative to the $T = 0.26$ K curve. (c) Temperature dependence of the width and height of the switching region, normalized to their maximum values, is plotted as a function of temperature. The gray line is a mean field magnetization for $S = 7/2$ and $T_c = 1.5$ K.

the lateral domain size ∼20 nm; see an extended TEM image [30]. At $H = 0$ and $T < T_N$ EuSe is in an AFM state and we anticipate formation of magnetic domain walls (DWs) between physical domains. The measured conductance <5 nS across the EuSe film includes transport through the bulk and along the DWs. Thus 40 μS jumps observed in magnetoresistance, Fig. 4, cannot originate from the transport through the EuSe layer. At the same time, these jumps are reminiscent of transport response in conducting magnetic materials to the reconstructions of magnetic domains. As we show in [30], domain walls, formed between adjacent AFM domains, may have extended regions of varying polarization. If conductivity of the TSSs depends on the orientation of the adjacent AFM layer, the abrupt switchings of resistance at high magnetic fields can be attributed to the reconstructions of antiferromagnetic domains in the interfacial EuSe layer.

III. CONCLUSIONS

In this paper we present detailed studies of Bi$_2$Se$_3$/EuSe heterostructures using a combination of PNR, XRR, magnetometry, and electron transport techniques. Using simultaneous fitting of PNR and XRR data we found that magnetic response of an interfacial 2 nm layer of EuSe is highly suppressed compared to the bulk of the film, and that suppression does not depend on the magnetic phase of the bulk EuSe. Moreover, the observed suppression of magnetic response persists at least up to 25 K, five times above the Neél temperature of the bulk EuSe. The absence of a paramagnetic response in the interfacial layer is accompanied by the absence of a ferromagnetic signal in SQUID magnetometry. Transport measurements reveal sharp resistance changes at high magnetic fields, which are consistent with a transport response to an abrupt reconstruction of magnetic domains. All of these observables are consistent with formation of a high-T_N antiferromagnetic layer in EuSe close to the Bi$_2$Se$_3$/EuSe

interface. This layer remains antiferromagnetically ordered up to very high magnetic fields and may be responsible for the observed magnetoresistance switching, attributed to domain reconstruction. A theoretical understanding of the interfacial exchange that leads to the formation of an AFM interfacial layer, as well as an understanding of how such an exchange affects transport in TSSs, requires further investigation.

[1] M. Z. Hasan and J. E. Moore, Three-dimensional topological insulators, Annu. Rev. Condens. Matter Phys. **2**, 55 (2011).

[2] Y. Deng, Y. Yu, M. Z. Shi, Z. Guo, Z. Xu, J. Wang, X. H. Chen, and Y. Zhang, Quantum anomalous Hall effect in intrinsic magnetic topological insulator $MnBi_2Te_4$, Science **367**, 895 (2020).

[3] C.-Z. Chang, J. Zhang, X. Feng, J. Shen, Z. Zhang, M. Guo, K. Li, Y. Ou, P. Wei, L.-L. Wang, Z.-Q. Ji, Y. Feng, S. Ji, X. Chen, J. Jia, X. Dai, Z. Fang, S.-C. Zhang, K. He, Y. Wang *et al.*, Experimental observation of the quantum anomalous Hall effect in a magnetic topological insulator, Science **340**, 167 (2013).

[4] J. Liu and T. Hesjedal, Magnetic topological insulator heterostructures: A review, Adv. Mater. **35**, 2102427 (2021).

[5] X. Hao, J. S. Moodera, and R. Meservey, Spin-filter effect of ferromagnetic europium sulfide tunnel barriers, Phys. Rev. B **42**, 8235 (1990).

[6] P. Wei, F. Katmis, B. A. Assaf, H. Steinberg, P. Jarillo-Herrero, D. Heiman, and J. S. Moodera, Exchange-coupling-induced symmetry breaking in topological insulators, Phys. Rev. Lett. **110**, 186807 (2013).

[7] Q. I. Yang, M. Dolev, L. Zhang, J. Zhao, A. D. Fried, E. Schemm, M. Liu, A. Palevski, A. F. Marshall, S. H. Risbud, and A. Kapitulnik, Emerging weak localization effects on a topological insulator-insulating ferromagnet (Bi_2Se_3-EuS) interface, Phys. Rev. B **88**, 081407(R) (2013).

[8] L. D. Alegria, H. Ji, N. Yao, J. J. Clarke, R. J. Cava, and J. R. Petta, Large anomalous Hall effect in ferromagnetic insulator-topological insulator heterostructures, Appl. Phys. Lett. **105**, 053512 (2014).

[9] M. Lang, M. Montazeri, M. C. Onbasli, X. Kou, Y. Fan, P. Upadhyaya, K. Yao, F. Liu, Y. Jiang, W. Jiang, K. L. Wong, G. Yu, J. Tang, T. Nie, L. He, R. N. Schwartz, Y. Wang, C. A. Ross, and K. L. Wang, Proximity induced high-temperature magnetic order in topological insulator - ferrimagnetic insulator heterostructure, Nano Lett. **14**, 3459 (2014).

[10] W. Yang, S. Yang, Q. Zhang, Y. Xu, S. Shen, J. Liao, J. Teng, C. Nan, L. Gu, Y. Sun, K. Wu, and Y. Li, Proximity effect between a topological insulator and a magnetic insulator with large perpendicular anisotropy, Appl. Phys. Lett. **105**, 092411 (2014).

[11] Z. Jiang, C.-Z. Chang, C. Tang, P. Wei, J. S. Moodera, and J. Shi, Independent tuning of electronic properties and induced ferromagnetism in topological insulators with heterostructure approach, Nano Lett. **15**, 5835 (2015).

[12] F. Katmis, V. Lauter, F. S. Nogueira, B. A. Assaf, M. E. Jamer, P. Wei, B. Satpati, J. W. Freeland, I. Eremin, D. Heiman, P. Jarillo-Herrero, and J. S. Moodera, A high-temperature ferromagnetic topological insulating phase by proximity coupling, Nature (London) **533**, 513 (2016).

[13] X. Che, K. Murata, L. Pan, Q. L. He, G. Yu, Q. Shao, G. Yin, P. Deng, Y. Fan, B. Ma, X. Liang, B. Zhang, X. Han, L. Bi, Q.-H. Yang, H. Zhang, and K. L. Wang, Proximity-induced magnetic order in a transferred topological insulator thin film on a magnetic insulator, ACS Nano **12**, 5042 (2018).

[14] Y. T. Fanchiang, K. H. M. Chen, C. C. Tseng, C. C. Chen, C. K. Cheng, S. R. Yang, C. N. Wu, S. F. Lee, M. Hong, and J. Kwo, Strongly exchange-coupled and surface-state-modulated magnetization dynamics in Bi_2Se_3/yttrium iron garnet heterostructures, Nat. Commun. **9**, 223 (2018).

[15] V. M. Pereira, S. G. Altendorf, C. E. Liu, S. C. Liao, A. C. Komarek, M. Guo, H.-J. Lin, C. T. Chen, M. Hong, J. Kwo, L. H. Tjeng, and C. N. Wu, Topological insulator interfaced with ferromagnetic insulators: Bi_2Se_3 thin films on magnetite and iron garnets, Phys. Rev. Mater. **4**, 064202 (2020).

[16] H. Wang, Y. Liu, P. Wu, W. Hou, Y. Jiang, X. Li, C. Pandey, D. Chen, Q. Yang, H. Wang, D. Wei, N. Lei, W. Kang, L. Wen, T. Nie, W. Zhao, and K. L. Wang, Above room-temperature ferromagnetism in wafer-scale two-dimensional van der Waals Fe_3GeTe_2 tailored by a topological insulator, ACS Nano **14**, 10045 (2020).

[17] A. E. L. Allcca, X.-C. Pan, I. Miotkowski, K. Tanigaki, and Y. P. Chen, Gate-tunable anomalous Hall effect in stacked van der Waals ferromagnetic insulator–topological insulator heterostructures, Nano Lett. **22**, 8130 (2022).

[18] T. Bhowmick, S.-K. Jerng, J. H. Jeon, S. B. Roy, Y. H. Kim, J. Seo, J. S. Kim, and S.-H. Chun, Suppressed weak antilocalization in the topological insulator Bi_2Se_3 proximity coupled to antiferromagnetic NiO, Nanoscale **9**, 844 (2017).

[19] L. Pan, A. Grutter, P. Zhang, X. Che, T. Nozaki, A. Stern, M. Street, B. Zhang, B. Casas, Q. L. He, E. S. Choi, S. M. Disseler, D. A. Gilbert, G. Yin, Q. Shao, P. Deng, Y. Wu, X. Liu, X. Kou, S. Masashi *et al.*, Observation of quantum anomalous Hall effect and exchange interaction in topological insulator/antiferromagnet heterostructure, Adv. Mater. **32**, 2001460 (2020).

[20] A. I. Figueroa, F. Bonell, M. G. Cuxart, M. Valvidares, P. Gargiani, G. van der Laan, A. Mugarza, and S. O. Valenzuela, Absence of magnetic proximity effect at the interface of Bi_2Se_3 and $(Bi, Sb)_2Te_3$ with EuS, Phys. Rev. Lett. **125**, 226801 (2020).

[21] J. A. Krieger, Y. Ou, M. Caputo, A. Chikina, M. Döbeli, M.-A. Husanu, I. Keren, T. Prokscha, A. Suter, C.-Z. Chang, J. S. Moodera, V. N. Strocov, and Z. Salman, Do topology and ferromagnetism cooperate at the EuS/Bi_2Se_3 interface? Phys. Rev. B **99**, 064423 (2019).

[22] H. L. Meyerheim, A. Ernst, K. Mohseni, A. Polyakov, I. V. Maznichenko, P. A. Buczek, A. Coati, and S. S. P. Parkin, Structure and magnetism of EuS on Bi_2Se_3(0001), Phys. Status Solidi B **258**, 2000290 (2020).

[23] M. Li, Q. Song, W. Zhao, J. A. Garlow, T.-H. Liu, L. Wu, Y. Zhu, J. S. Moodera, M. H. W. Chan, G. Chen, and C.-Z. Chang, Dirac-electron-mediated magnetic proximity effect in topological insulator/magnetic insulator heterostructures, Phys. Rev. B **96**, 201301(R) (2017).

[24] J. Kim, K.-W. Kim, H. Wang, J. Sinova, and R. Wu, Understanding the giant enhancement of exchange interaction in Bi_2Se_3-EuS heterostructures, Phys. Rev. Lett. **119**, 027201 (2017).

[25] S. Eremeev, V. Menshov, V. Tugushev, and E. Chulkov, Interface induced states at the boundary between a 3D topological insulator Bi_2Se_3 and a ferromagnetic insulator EuS, J. Magn. Magn. Mater. **383**, 30 (2015).

[26] D. Tristant, I. Vekhter, V. Meunier, and W. A. Shelton, Partial charge transfer and absence of induced magnetization in $EuS(111)/Bi_2Se_3$ heterostructures, Phys. Rev. B **104**, 075128 (2021).

[27] V.-C. Lee and L. Liu, Exchange mechanism in europium compounds, Phys. Rev. B **30**, 2026 (1984).

[28] A. Mauger and C. Godart, The magnetic, optical, and transport properties of representatives of a class of magnetic semiconductors: The europium chalcogenides, Phys. Rep. **141**, 51 (1986).

[29] Y. Wang, X. Liu, S.-K. Bac, J. Wang, J. K. Furdyna, B. A. Assaf, M. Zhukovskyi, T. Orlova, V. Lauter, N. R. Dilley, and L. P. Rokhinson, Epitaxial growth and magnetic characterization of EuSe thin films with various crystalline orientations, J. Appl. Phys. **131**, 055302 (2022).

[30] See Supplemental Material at http://link.aps.org/supplemental/10.1103/PhysRevB.108.195308 for a detailed description of methods, additional information on PNR measurements, EuSe magnetization data, high-resolution TEM images, transport properties of the EuSe films, and micromagnetic modeling of AFM domain walls.

[31] R. T. Lechner, G. Springholz, T. U. Schülli, J. Stangl, T. Schwarzl, and G. Bauer, Strain induced changes in the magnetic phase diagram of metamagnetic heteroepitaxial EuSe/PbSe$_{1-x}$Te$_x$ multilayers, Phys. Rev. Lett. **94**, 157201 (2005).

[32] D. Korneev, V. Pasyuk, A. Petrenko, and H. Jankovski, Absorbing sublayers and their influence on the polarizing efficiency of magnetic neutron mirrors, Nucl. Instrum. Methods Phys. Res., Sect. B **63**, 328 (1992).

[33] V. Lauter-Pasyuk, Neutron grazing incidence techniques for nano-science, https://www.neutron-sciences.org/articles/sfn/olm/2007/02/sfn2007009/sfn20070s9.pdf.

[34] H. Lauter, V. Lauter, and B. Toperverg, Reflectivity, off-specular scattering, and GI-SAS, in *Polymer Science: A Comprehensive Reference* (Elsevier, 2012), pp. 411–432.

[35] K. Prokeš, C. Luo, H. Ryll, E. Schierle, D. Marchenko, E. Weschke, F. Radu, R. Abrudan, V. V. Volobuev, G. Springholz, and O. Rader, Search for enhanced magnetism at the interface between Bi$_2$Se$_3$ and EuSe, Phys. Rev. B **103**, 115438 (2021).

[36] S. Hikami, A. I. Larkin, and Y. Nagaoka, Spin-orbit interaction and magnetoresistance in the two dimensional random system, Prog. Theor. Phys. **63**, 707 (1980).

[37] See http://energy.gov/downloads/doe-public-access-plan.